DYNAMICS OF MOLECULAR OXYGEN IN MICELLAR SOLUTIONS

Nicholas J. TURRO, Masayuki AIKAWA
Chemistry Department, Columbia University, New York, New York 10027, USA

and

Ahmad YEKTA
Chemistry Department, Arya-Mehr Univesrity of Technology, Tehran, Iran

Received 23 March 1979

Fluorescence quenching by molecular oxygen has been employed to estimate dynamic parameters and solubility characteristics of molecular oxygen in micelle forming detergent solutions. A kinetic model which assumes that oxygen quenching occurs only in the micellar phase is employed to analyze the data.

1. Introduction

Molecular oxygen is a general and effective quencher of the fluorescence of aromatic hydrocarbons [1]. The quenching process is commonly diffusion controlled in homogeneous solution, requiring that quenching within the "solvent cage" [2] occurs with an efficiency close to unity. In two (or multiphase) pseudo-homogeneous aqueous solutions (micelle containing detergent solutions, solutions containing protein membranes and other macro biomolecules) the observed efficiency and reactivity of oxygen quenching will depend on the partitioning of molecular oxygen in the various phases, the lifetimes of the excited quencher and the dynamics of entrance, exit and quenching interaction of the oxygen molecule in an "effective quenching volume" [3] about the quencher. Thus, in extreme situations quenching (1) can be very effective if the oxygen molecule and quencher are "pre-complexed" and confined to a small volume in a given phase or (2) can become very inefficient if the quencher and the molecular oxygen are in separate phases and volumes of space and the rate of penetration of oxygen into an "effective quenching volume" is slow compared to the decay rate of the excited quencher.

Previous work on aromatic hydrocarbon fluorescence quenching by molecular oxygen in aqueous solutions has been limited in scope, presumably in part because of the low solubility of aromatic hydrocarbons and of molecular oxygen in aqueous solutions. The maximum concentration of aromatic hydrocarbons attainable in micelle containing aqueous solutions of detergents is much greater than that attainable in water. The oxygen concentration may be enhanced by simply increasing the pressure of oxygen in the system [4].

Evidence has been presented that molecular oxygen readily penetrates micelle [5] ‡ and membrane [7] boundaries. The mechanism of penetration of molecular oxygen across such boundaries is potentially of great significance for important biological processes such as respiration and photodynamic effects [8].

The "observed" rate constant for quenching of fluorescent probes by molecular oxygen in solutions containing proteins [9], DNA [10], micelles [5,6] and vesicles [7] is smaller than that observed for the same probes in homogeneous solution. These results have been interpreted in terms of a smaller "effective" concentration of oxygen in the phase or aggregates containing the probe, in terms of a smaller rate constant for quenching interaction or some combination of both factors. The ability of association to "protect" excited

‡ It also appears that singlet oxygen can readily penetrate micelles: see ref. [6].

probes from oxygen quenching is strikingly demonstrated by the ready observation of *phosphorescence* from organic molecules in micelle containing detergent solutions [11].

Information on the solubilization, entry and exit of molecular oxygen into and out of micelles produced in detergent solution is potentially available from an investigation of the time resolved measurement of fluorescence lifetime of a micellized probe as a function of oxygen pressure. We report here a study of the oxygen quenching of 1,5-dimethylnaphthalene fluorescence in micelle containing detergent solutions of hexadecyltrimethyl-ammonium bromide (HDTBr) and sodium dodecyl sulfate (SDS). A kinetic analysis of our data allows an estimation of dynamic and solubility parameters of molecular oxygen in this "two phase" system.

2. Experimental strategy and kinetic model

The experimental method employed involves time correlated single photon counting [12] measurement of the fluorescence decay of the probe as a function of oxygen pressure [9,10]. At low partial pressure (< 1 atm) of oxygen, the observed fluorescence decay (fig. 1a) is exponential within experimental error and equal to that of the fluorescence decay of the probe in thoroughly degassed solution (fig. 1b). However, at higher pressures of oxygen (> 1 atm) the fluorescence decay (figs. 1c, 1d and 1e) is initially non-exponential ("short time decay", τ_s) but eventually becomes exponential ("long time decay", τ_l). Significantly, the "long time decay" *is shorter than the decay in degassed solution*. We interpret the short time decay in terms of "static" fluorescence quenching in micelles that contain both an oxygen molecule and an excited probe molecule at the end of the excitation pulse ($t = 0$); we interpret the long time decay in terms of "dynamic" fluorescence quenching that occurs at the end of the excitation pulse ($t = 0$) that is due to diffusion of oxygen molecules (initially located in the aqueous phase) into a micelle containing an excited probe molecule.

We handle the experimental data by employing scheme 1 as a model. This model assumes that a combination of static and dynamic quenching of probe fluorescence operates. We relate the experimental data to the following micellar parameters [4]: $\langle O_2 \rangle$, the average occupancy number of oxygen molecules in a micelle

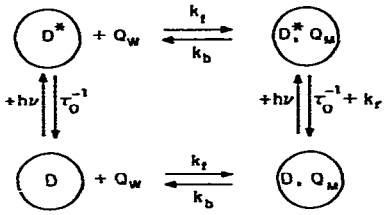

Scheme 1. Schematic representation of the model for quenching of a luminescent probe by a quencher which is present in both aqueous (Q_W) and micellar (Q_M) phases.

(based on Poisson statistics); α, the efficiency of quenching of the excited probe by an oxygen molecule once it is in a micelle; k_f, the rate of entry of oxygen into the micelle; and, k_b, the rate of exit of oxygen from the micelle by the following expression [13]:

$$\ln[I(t)/I(0)] = -(t/\tau + \langle O_2 \rangle \alpha^2) + \langle O_2 \rangle \alpha^2 \exp[-(k_r + k_b)t]. \quad (1)$$

If $\langle O_2 \rangle$ is known, then this equation can be solved for α and $(k_r + k_b)$. Knowledge of these quantities then al-

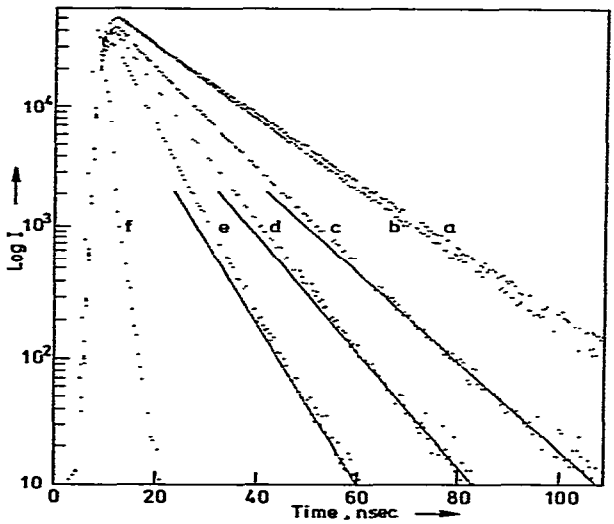

Fig. 1. Fluorescence decay modes of 1,5-DMN under various O_2 pressures. O_2 pressures are: (a) degassed (10^{-5} Torr); (b) 0.2; (c) 1.36; (d) 2.72; (e) 5.44 atm, respectively. Curve (f) represents the shape of D_2 flash lamp (half width is ≈ 2.1 ns).

lows evaluation of the individual rate constants k_f, k_b, and k_r.

From eq. (1) in the long time domain one obtains

$$\{\ln[I(t)/I(0)]\}_{t\to\infty} \approx -(t/\tau + \langle O_2\rangle\alpha^2), \qquad (2)$$

so that for this limit the slope of a plot of eq. (2) furnishes the fluorescence lifetime τ in the presence of diffusional quenching and extrapolation to the intercept from long time to $t = 0$ yields $\langle O_2\rangle\alpha^2$.

The plots of the latter values of $\langle O_2\rangle\alpha^2$ versus oxygen pressure P_{O_2} are shown in fig. 2. The good linearity of the plot validates the assumption that $\ln[I(t)/I(0)]$ is proportional to $\langle O_2\rangle$. The values of $\langle O_2\rangle$ for HDTBr and SDS micelles as a function of P_{O_2} were evaluated from solubility measurements of Matheson and King [4]. These authors demonstrated experimentally that the concentration of micellized oxygen $[O_2]_{mic}$ is given by

$$[O_2]_{mic} = a([\text{HDTBr}] - \text{CMC})P_{O_2}, \qquad (3)$$

where $a = 1.4 \times 10^{-3}$ atm^{-1} for (HDTBr) and 1.04×10^{-3} atm^{-1} for (SDS). The relationship between the average micelle aggregation number $\bar{n}$ and the total micelle concentration, [M], alows eq. (3) to be rewritten as

$$[O_2]_{mic} = a\bar{n}[M]P_{O_2}. \qquad (4)$$

Furthermore, since $\langle O_2\rangle = [O_2]_{mic}/[M]$ where [M] is the concentration of micelles, we have

$$\langle O_2\rangle = a\bar{n}P_{O_2}, \qquad (5)$$

so that the slope of the plot in fig. 2 is identified as $\alpha^2 a\bar{n}$. From the reported values [14] of $\bar{n}$ the representative values $\bar{n} = 80$ for HDTBr and $\bar{n} = 60$ for SDS.

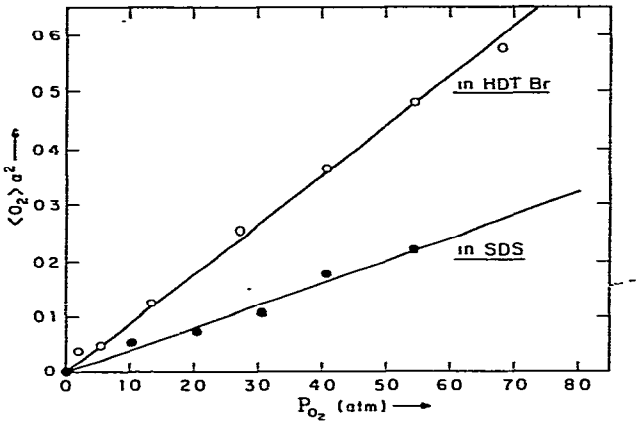

Fig. 2. A plot of $\langle O_2\rangle\alpha_r^2$ against O_2 pressure for HDTBr and SDS micellar solution. The slope gives the value of $\alpha^2 a\bar{n}$.

We derive a value of $\alpha = 0.89 \pm 0.15$ (HDTBr) and 0.80 ± 0.17 (SDS).

Rearrangement of eq. (1) yields

$$1 + \frac{\ln[I(t)/I(0)] + t/\tau}{\langle O_2\rangle\alpha^2} = \exp[-(k_r + k_b)t], \qquad (6)$$

The logarithmic plots of the above function yield $k_r + k_b = (4.6 \pm 0.5) \times 10^7$ s^{-1} (HDTBr) and $(5.3 \pm 0.7) \times 10^7$ s^{-1} (SDS) and are independent of pressure. Our results place an upper limit to the sum $k_r + k_b$, and also limit the values of the individual rate constants (table 1). However, since the experimental error and scatter in reported values [14] of $\bar{n}$ in determining α is estimated to be $\approx 20\%$, ev ation of the values of

Table 1
Summary of parameters derived from fluorescence quenching in micellar solutions

Parameter	Micelles	
	HDTBr	SDS
entrance rate constant, k_f	$(1.3 \pm 0.2) \times 10^{10}$ M^{-1} s^{-1}	$(1.4 \pm 0.2) \times 10^{10}$ M^{-1} s^{-1}
exit rate constant, k_b	$< (4.6 \pm 0.5) \times 10^7$ s^{-1}	$< (5.3 \pm 0.7) \times 10^7$ s^{-1}
residence time, τ_m	$< 22 \times 10^{-9}$ s	$< 19 \times 10^{-9}$ s
"static quenching constant, k_r	$< (4.6 \pm 0.5) \times 10^7$ s^{-1}	$< (5.3 \pm 0.7) \times 10^7$ s^{-1}
quenching efficiency, α	0.89 ± 0.15	0.80 ± 0.17
equilibrium constant, $K_{eq} \equiv k_f/k_b$	$(2.8 \pm 0.3) \times 10^2$ M^{-1}	$(2.6 \pm 0.34) \times 10^2$ M^{-1}

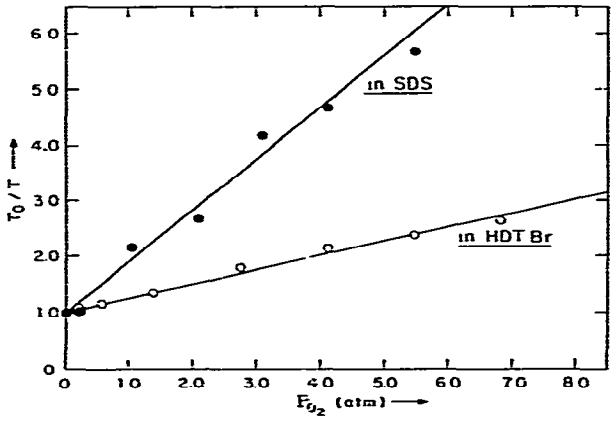

Fig. 3. A plot of τ_0/τ against O_2 pressure for HDTBr and SDS micellar solution. The slope gives $k_q\tau_0$.

individual rate constants is subject to a large inaccuracy. Nevertheless the limiting residence time of O_2 in HDTBr and SDS micelles is $>200 \times 10^{-9}$ and $>91 \times 10^{-9}$ s, respectively. These correspond to limiting exit rates of $<4.6 \times 10^7$ s^{-1} and $<5.3 \times 10^7$ s^{-1} for HDTBr and SDS, respectively.

The relation between the diffusional limited fluorescence lifetime and the oxygen concentration in the water phase is given by [10,13]

$$\tau^{-1} = \tau_0^{-1} + k_f[O_2]_w. \quad (7)$$

Since Matheson and King [4] demonstrated that $[O_2]_w = 1.39 \times 10^{-3} P_{O_2}$ we have

$$\tau^{-1} = \tau_0^{-1} + k_f(1.39 \times 10^{-3})P_{O_2}. \quad (8)$$

Fig. 3 shows a plot of τ_0/τ versus P_{O_2} for the HDTBr and SDS systems. The slopes yield the forward rate constant of oxygen association with the micelle $k_f = 1.3 \times 10^{10}$ M^{-1} s^{-1} (HDTBr) and 1.4×10^{10} M^{-1} s^{-1} (SDS).

Unlike the values of k_b and k_r, upon which we can only place limits, the values of k_f are available within a precision of $\approx 20\%$. Knowledge of the values of k_f together with the limiting values of k_b allow the estimation of a limiting value of $K_{eq} \equiv k_f/k_b$:

$$K_{eq}(\text{HDTBr}) \geq 2.8 \times 10^2 \text{ M}^{-1}, \quad (9)$$

$$K_{eq}(\text{SDS}) \geq 2.6 \times 10^2 \text{ M}^{-1}. \quad (10)$$

3. Discussion: comparison with related published data

The question arises as to whether the numbers derived from our analysis are reasonable and consistent with the magnitudes of analogous parameters derived from other systems.

The value of the entrance rate constants 1.3×10^{10} M^{-1} s^{-1} (HDTBr) and 1.4×10^{10} M^{-1} s^{-1} (SDS) are comparable to those derived from fluorescence quenching by oxygen. For example, values of 8.3×10^9 M^{-1} s^{-1} (HDTBr) and 9.2×10^9 M^{-1} s^{-1} (SDS) were reported for the total "bulk" oxygen quenching of pyrene monomer fluorescence. The long inherent lifetime of pyrene fluorescence (≈ 200 ns in HDTBr and ≈ 450 ns in SDS, respectively) probably allows oxygen escape from the micelle to be competitive with oxygen quenching; therefore, the observed quenching constant is somewhat lower than that for diffusion of oxygen into the micelle.

The value of the rate constant for interaction (quenching) of excited 1,5-dimethyl naphthalene is expected to be of the order of that for intramicellar encounter of an oxygen molecule and an excited naphthalene molecule. From the values of the reported microviscosities of HDTBr and SDS micelles (39 and 9 cP, respectively) [15], a micelle radius of ≈ 20 Å and an effective radius of the probe of ≈ 3.0 Å, a value of $(1-5) \times 10^7$ s^{-1} is calculated from diffusion theory for the encounter rate [16]. An experimental value of $\approx 10^7$ s^{-1} has been evaluated for the intramicellar encounter of two pyrene molecules in an anionic micelle [17]. Finally, a value of $\approx 6 \times 10^7$ s^{-1} has been evaluated for the rate of intramolecular excimer formation of 1,3-di-α-naphthylpropane in HDTBr micelles [18]. All these data suggest micellar interaction rate constants of the order of 10^7–10^8 s^{-1} for the systems studied. Our derived value of $\lesssim 4.6 \times 10^7$ s^{-1} or $\lesssim 5.3 \times 10^7$ s^{-1} is comparable to literature estimates.

The magnitude of $\alpha \approx 1$ is consistent with results from homogeneous solution where O_2 is found to quench the fluorescence of aromatic hydrocarbons at close to the diffusional limit.

Finally, the limit of K_{eq} of $\approx 3 \times 10^2$ M^{-1} implies a higher solubility of O_2 in the micellar phase relative to the aqueous phase (on a molar basis). This result is consistent with the observation that O_2 is generally an order of magnitude more soluble in organic solvents than it is in water [5–7]. The comparable value of K_{eq}

for HDTBr and SDS is consistent with a recent investigation of the oxygen quenching of naphthalene fluorescence in aqueous solutions of these two detergents [19].

4. Experimental

HDTBr and SDS were washed several times with ether and recrystallized from water three times. DMN was purified by sublimation in vacuo. Oxygen (Airco, Inc.) and 40% oxygen/nitrogen (Matheson Gas Products) for calibration or for lower O_2 pressure were used.

Transient decay curves of micellar solution under high oxygen pressure were measured using the time-correlated single-photon counting technique [12]. The flash lamp was operated at a high voltage of 4.5 kV and repetition of ≈ 15 kHz. Deuterium at 1/2 atm pressure was used as a flash gas. The gas discharged flash lamp gave a pulse with a half-width of about 2.1–2.6 ns. Interference band pass filters (Corion Instruments Corp.) were used to select wavelengths from the exciting light. These filters transmitted 30% of the incident radiation at its wavelength of maximum 311.2 or 304.2 nm with a 10 nm half-width. Sample fluorescence of appropriate wavelength was selected with an American ISA, Inc. 1/10 meter monochromator. A RCA photomultiplier (C31034A02) with refrigerated chamber (Research Inc. TE-104-RF) was used as the photodetector. Fluorescence intensities were adjusted at 350–700 counts/s. The dark noise (adjusted via a discriminator) was about 15 ± 10 counts/s.

The high pressure apparatus was placed inside of a "dark box" and adjusted in the light path of the D_2 lamp. The apparatus consists of a thick-walled (1/2 in.) cylindrical stainless steel vessel which has optical quartz windows on the three sides and has a brass jacket combined with temperature-controlled water bath [10]. A cell holder was mounted on the bottom of the vessel. The high pressure vessel rested on a variable magnetic stirrer, allowing the agitation by a magnetic stirring bar in the cell set in the cell holder to be controlled externally. An inlet line to the vessel was connected to a gas manifold through a needle valve allowing the vessel to be loaded with the gas desired. A Boudon gauge (Matheson), accurate to 0.25% of full scale, was used to record the loaded pressure. An exit line was also attached to the vessel through a needle valve and allows the gas to be released.

Before loading the vessel with desired pressure, the air of the vessel was replaced several times with oxygen or the mixture gas by controlling the inlet and outlet needle valves. Then the gas was introduced over the vessel at the desired pressure, and the solution in the cell was allowed to equilibrate with the dense gas for a minimum of two hours with stirring. The stirrer was shut off, and the transient decay curve of the solution was measured.

To test the accuracy of the "nominal" pressure observed in running experiments, the rate constant for quenching of fluorescence of aqueous solutions of 1,5-DMN was measured. Pressures of a mixture of O_2/N_2 (= 40/60) up to 100 lb/in^2 were employed. The decay of 1,5-DMN fluorescence in H_2O consisted of a single exponential throughout the range of O_2 pressures studied. The solubility of molecular oxygen in water was reported as

$$[O_2]_W = bP_{O_2}, \qquad (11)$$

where $b = 1.39 \times 10^{-3}$ mol ℓ^{-1} atm^{-1} [4]. Fig. 4 shows the reciprocal of 1,5-DMN lifetime as a function of $[O_2]$. From eq. (11) and the slope of fig. 4, a quenching rate constant of oxygen in water $k_q = 1.43 \times 10^{10}$ M^{-1} s^{-1} is derived. This value is in good agreement with the oxygen quenching rate constant of various fluorophores in aqueous solutions [10].

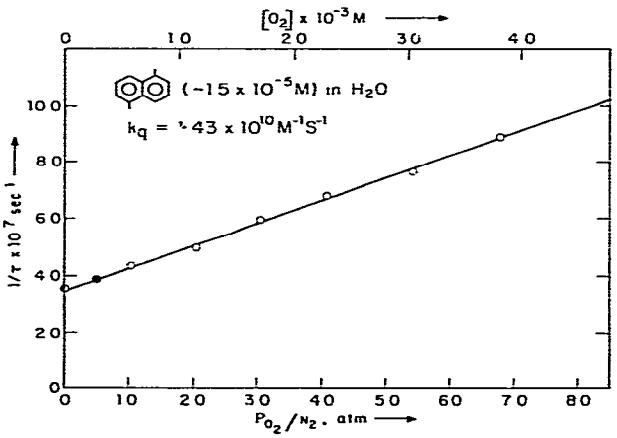

Fig. 4. Stern–Volmer plot for quenching of 1,5-DMN fluorescence in H_2O solution as a function of O_2 pressures. Degassed (10^{-5} mm Hg) (•), atomospheric condition (•) and O_2/N_2 mixed gas (○).

DOCKET ALARM

Explore Litigation Insights

Docket Alarm provides insights to develop a more informed litigation strategy and the peace of mind of knowing you're on top of things.

Real-Time Litigation Alerts

Keep your litigation team up-to-date with **real-time alerts** and advanced team management tools built for the enterprise, all while greatly reducing PACER spend.

Our comprehensive service means we can handle Federal, State, and Administrative courts across the country.

Advanced Docket Research

With over 230 million records, Docket Alarm's cloud-native docket research platform finds what other services can't. Coverage includes Federal, State, plus PTAB, TTAB, ITC and NLRB decisions, all in one place.

Identify arguments that have been successful in the past with full text, pinpoint searching. Link to case law cited within any court document via Fastcase.

Analytics At Your Fingertips

Learn what happened the last time a particular judge, opposing counsel or company faced cases similar to yours.

Advanced out-of-the-box PTAB and TTAB analytics are always at your fingertips.

API

Docket Alarm offers a powerful API (application programming interface) to developers that want to integrate case filings into their apps.

LAW FIRMS
Build custom dashboards for your attorneys and clients with live data direct from the court.

Automate many repetitive legal tasks like conflict checks, document management, and marketing.

FINANCIAL INSTITUTIONS
Litigation and bankruptcy checks for companies and debtors.

E-DISCOVERY AND LEGAL VENDORS
Sync your system to PACER to automate legal marketing.